Journal of Plant Stress Physiology 2026, 12: 32-42
https://doi.org/10.25081/jpsp.2026.v12.9807

Research Article

The synthesized nanocomposite, rGO/SiO_2/ZnO, mitigates salinity impacts on soybean

Mamdouh M. Nemat Alla[1]*, Enas G. Badran[1], Manal A. Abdelhamid[2], Nemat M. Hassan[1], Mohamed M. El-Zahed[1]

[1]*Botany Department, Faculty of Science, Damietta University, PO 34517 New Damietta, Egypt*
[2]*Botany Department, Faculty of Science, Sebha University, Libya*

(Received: November 20, 2025; Revised: February 10, 2026; Accepted: February 13, 2026; Published: March 24, 2026)
*Corresponding author: Mamdouh M. Nemat Alla, E-mail: mamnematalla@du.edu.eg

Abstract

Soybean is an important crop in Egypt; however, the domestic supply is insufficient due to the limited agricultural areas despite the huge area of saline soils. So, utilizing these saline soils to cultivate soybeans, while increasing its tolerance to salinity by external assistance, can increase its productivity and close the food gap. Using the nanoparticles (NPs) is promising as potential solution in this field. For this purpose, the rGO/SiO_2/ZnO nanocomposite (NC) was successfully synthesized from reduced graphene oxide, silicon dioxide, and zinc oxide NPs in combination with soybean extract to be used as seed priming to mitigate salinity impacts. The synthesized NC is characterized with an absorption peak at 354 nm, indicating the annealing of ZnO NPs and SiO_2 NPs on the GO sheets with a positive charge (+30.9±10.4 mV) and the NPs were rod-shaped particles with an average size ranging from 64 to 78 nm. Soybean seedlings suffered from salinity stress (NaCl at 100, or 200 mM) as significant reductions in growth parameters coincided with decreasing phenolics, protein, and activities of peroxidase and catalase. However, priming seeds in the synthesized NC effectively mitigated the impacts of NaCl, restoring parameter values close to -and even exceeded- the control. Among the used concentrations of the NC, 150 and 300 μg L^{-1} were more effective than 50 μg L^{-1} but 500 μg L^{-1} was inappropriate and seemed to synergize the impacts of salinity. These results suggest that salinity has negative impacts on soybean while using the rGO/SiO_2/ZnO NC is a highly promising safe and efficient protectant for enhancing soybean's resilience when used at the concentrations 150 and 300 μg L^{-1}. The novelty of the rGO/SiO_2/ZnO NC tri-component architecture as safe and efficient seed priming agent has been demonstrated, this knowledge might be useful for understanding the responses of the plant cells to modulate NaCl tolerance in future researches.

Keywords: Antioxidant enzymes, Growth parameters, Phenolics, Protein, Stress tolerance

Introduction

Soybean occupies a main position among agricultural crops, being the most vital source of proteins and vegetable oil (Budran *et al.,* 2023). Soy proteins are the primary source of plant-based proteins containing well-balanced essential amino acids except for sulfur-containing ones (Qin *et al.,* 2022; Budran *et al.,* 2023). Despite its utmost importance in Egypt, soybean productivity is insufficient to meet the need therefore; strategies have to include increasing its productivity. Enlarging soybean cultivation might be a solution for food security, import reliance, and economic diversification in Egypt (Naser *et al.,* 2024). Given the importance of the soybean crop in addition to the urgent and pressing need for it, and given the limited availability of arable lands, as well as the vast areas of saline and neglected lands, it is necessary to utilize this abundance of saline and neglected land for soybean cultivation, but with the use of external assistance.

Salinity negatively affects plant growth due to ion toxicity and water stress, which can lead to dehydration and increasing oxidative damage (Sarioğlu, 2025). Plant height, leaf number, and biomass (both shoot and root dry weight) are significantly reduced as salinity increases (Shah *et al.,* 2020). Plants experience increased oxidative damage, which can be measured by a decrease in antioxidant activity (Tripathi *et al.,* 2020) and an increase in the production of stress-related compounds (Naseem *et al.,* 2023). The hypothesis is that considering the great importance of soybean for human needs in addition to taking into account the existence of huge abundant and neglected saline areas, tolerance of soybean to salinity could be enhanced –to utilize these saline areas- by using safe and efficient formulation of nanoparticles (NPs) as an external supporter. Herein in the present work, an attempt was performed to synthesize an efficient nanocomposite (NC) from Zinc oxide (ZnO), silicon dioxide (SiO_2), and graphene oxide (GO) NPs in combination with soybean extract to alleviate the impact of salt stress. Adoption of nanotechnology in agriculture, being a fast-developing field, has gained considerable ground (Hofmann *et al.,* 2020). Rastogi *et al*. (2019) concluded that NPs are potential materials for the site-specific delivery of nucleotides, proteins and chemicals under *in vitro* conditions for achieving vital goals such as improving crop growth and yield as well as tolerance against stressful cues. NPs can mitigate salinity stress in plants by enhancing antioxidant defense, improving ion balance, and promoting overall growth and yield (Mohamed *et al.,* 2025).

Key mechanisms include ZnO and Si NPs boosting the activity of antioxidant enzymes and influencing ion transporters in plant cells (Rehman *et al.,* 2024) leading to less oxidative damage and improved plant performance under saline conditions. Zn supports enzymatic functions and ion homeostasis (Alsafran *et al.,* 2022), meanwhile, Si which is a critical component of crop production, especially in minimizing the negative impacts of oxidative, salinity,

and drought stresses (Seleiman *et al.,* 2019), is considered as quasi-essential for plant growth and development, and alleviates toxic effects caused by various environmental stresses in plants. Whilst GO enhances plant growth, nutrient absorption, and stress tolerance (Asadi *et al.,* 2025), improves chlorophyll content and water retention (Safkhan *et al.,* 2018) and can act as a fertilizer, a smart delivery system for nutrients and pesticides, and a tool for improving soil health as well as enhancing the antimicrobial properties (Baka & El-Zahed, 2023). These NPs increased plant stress tolerance by preserving critical physiological and biochemical functions (Zhan *et al.,* 2024).

Nanopriming can reduce the negative effects of salt stress by decreasing harmful compounds (Ochoa-Chaparro *et al.,* 2025), stimulate the production of antioxidant enzymes which help protect the plant from damage and induce the formation of nanopores in shoots, increase the expression of aquaporin genes, and speed up starch hydrolysis, all of which promote germination and early growth (Geremew *et al.,* 2025). Si-Zn nanocomposites increased yield in maize under saline field conditions (Shoukat *et al.,* 2025). Herein, the NC (rGO/SiO_2/ZnO) was successfully synthesized from SiO_2, ZnO and GO NPs in combination with soybean extract to be used for priming soybean seeds. The impacts of NaCl stress on growth characteristics, contents of phenolics and protein, and activities of peroxidase and catalase were investigated in soybean seedlings grown without or with the utilization of the NC. Hence, the objectives of this work were: 1) to declare the impacts of NaCl on soybean, 2) to synthesize a safe and effective NC (rGO/SiO_2/ZnO) from the NPs, rGO, SiO_2 and ZnO, and soybean extract to be used to support soybean under salinity, 3) to utilize the synthesized NC as seed priming for mitigating the impacts of NaCl on soybean, and 4) to distinguish the most effective concentration of the synthesized NC in assisting soybean.

Materials and methods

Preparation of soybean extract

Seeds of soybean [*Glycine max* (L.)] cultivar Giza 21 were obtained from the Agricultural Research Institute, Kafr El Sheikh, Egypt. Equally sized and healthy seeds were surface sterilized with 1% w/v sodium hypochlorite for 5 min and washed carefully with water, then soaked in water overnight. The seeds were cultivated in plastic pots (18 × 15 × 12 cm) containing clay: sand soil (2:1 w/w), approximately 2 cm-depth and spaced 5 cm apart and left in greenhouse at 25±2/14±2 °C, day/night temperature with a 12-h photoperiod at 420-460 µmol m^{-2} s^{-1} PPFD and received water (200 ml per pot) daily for 7 days followed by Long Ashton nutrient solution for 3 days. On the 12th day, fresh leaves were collected, cut into small pieces, ground and soaked in distilled water at 25 °C with continuous agitation at 150 rpm for 24 h. The mixture was filtered using Whatman filter paper No.1 followed by centrifugation at 4000 ×g for 20 min to obtain a clear extract and preserved in dark containers in a refrigerator for the biosynthesis of NPs.

Synthesis of NPs and the nanocomposite (rGO/SiO_2/ZnO)

ZnO NPs were synthesized according to the method of Umar *et al*. (2019). The plant extract (10 mL) was added dropwise onto 90 mL zinc nitrate (0.1 M) in a 250 mL Erlenmeyer flask with continuous stirring at 80 °C for 3 h. NaOH solution was added to maintain the pH between 9 and 10. With time, there was a discernible color change from yellowish-green to yellowish-white, indicating the production of NPs. The pale white precipitate of ZnO NPs was collected by centrifugation at 4000 ×g for 15 min, washed several times with distilled water, and dried in an oven at 70 °C for 8 h. The NPs were calcined in a muffle furnace at 550 °C for 5 h.

To green synthesize SiO_2 NPs, the soybean extract was combined with sodium silicate solution (1 mM, pH 6) in a 1:1 v/v mixing ratio and kept on a shaker at 150 rpm at room temperature overnight until the reaction solution color changes into brown. The generated NPs were filtered through Whatman filter paper No. 1. Calcination was allowed at 180 °C for 5 h for the formation of SiO_2 NPs (Al-Azawi *et al.,* 2019).

For the synthesis of the NC (rGO/SiO_2/ZnO), 0.1 GO powder was sonicated in 100 mL of ethylene glycol (Sigma Aldrich, 99%) for 2 h followed by the addition of 2 g of low-molecular weight polyacrylic acid (PAA) powder (Sigma Aldrich, mw ¼ 1800) to form PAA-GO. SiO_2 NPs (0.1 g) were added to the PAA-GO suspension and stirred for 20 min at 90 °C. The solution was filtered and cleaned to eliminate any potential surplus of undispersed SiO_2 or PAA that was not trapped in the GO matrix. The resulting product (SiO_2/GO) was dried at 50 °C for 12 h (Maroni *et al.,* 2014). ZnO NPs solution (1% in distilled water) was prepared, sonicated for an h, mixed with SiO_2/GO solution (1% in distilled water) at a mixing ratio 1:1 v/v with continuous stirring for 20 min at 95 °C to produce a gelatinous state. The final product NC, rGO/SiO_2/ZnO, was centrifuged and dried at 80 °C for 3 h (Jafari *et al.,* 2018).

Characterization of the rGO/SiO_2/ZnO NC

The synthesized ZnO NPs, SiO_2 NPs, and rGO/SiO2/ZnO NC were examined using Fourier transform infrared spectroscopy (FTIR, FT/IR-4100typeA) and a double beam UV–Vis spectrophotometer V-630 (JASCO, UK). The characteristics of rGO/SiO_2/ZnO were investigated using an X-ray diffractometer (model LabX XRD-6000, Shimadzu, Japan), a transmission electron microscope (TEM) device (200 kV, TEM JEOL JEM-2100, Japan), and a zeta potential analyzer (Malvern Zetasizer Nano-ZS90, Malvern, UK).

Growth conditions

Certified seeds of soybean [*Glycine max* (L.) Giza 21], obtained from Agricultural Research Institute, Kafr El Sheikh, Egypt were surface sterilized with 1% w/v sodium hypochlorite for 5 min, rinsed with water several times and primed overnight in the synthesized rGO/SiO_2/ZnO NC at the concentrations 0, 50, 150, 300 and 500 µg L^{-1}. The seeds were

cultivated in plastic pots (18 × 15 × 12 cm) containing clay: sand soil (2:1 w/w), approximately 2 cm-depth and spaced 5 cm apart and left in greenhouse at 25±2/14±2 °C, day/night temperature with a 12-h photoperiod at 420-460 µmol m^{-2} s^{-1} PPFD. All pots received water (200 mL per pot) daily for 7 days followed by Long Ashton nutrient solution for 3 days then the pots were divided into three groups for treatment with NaCl at 0, 100 mM, and 200 mM for the following 13 days. On the 24th day after sowing, seedlings were collected and separated into leaves, shoots and roots for the estimation of growth parameters. The new leaves and the upper parts were collected for the determination of the contents of phenolics and protein and of the activities of peroxidase and catalase.

Estimation of growth parameters

Fresh weights of leaves, shoots and roots were estimated then dried at 80 °C for 2 days for dry weight determinations. Water content was calculated on fresh weight basis. In addition, leaf area, shoot height, root length were calculated, as well as the ratios of fresh weight/dry weight for both shoots and roots and also of root/shoot for both fresh weight and length.

Determination of total phenolic contents

A known weight of fresh leaves (about 5 g) was homogenized in methanol: water (8:2, v: v) and centrifuged at 5000 ×g for 15 min. Total phenolic compounds were determined using Folin-Ciocalteau assay reagent (FC, 100 g of sodium tungstate and 25 g of sodium molybdate dissolved in 700 mL of distilled water) and gallic acid as a reference standard (Singleton & Rossi, 1965). Samples (1 mL) were mixed with 5 mL FC reagent, vortexed, left standing at room temperature for 5 min then 15 mL of Na_2CO_3 (7.5%) were added, mixed, and diluted to volume. After standing for 2 h in the dark at room temperature, the absorbance at 765 nm was determined against gallic acid as standard.

Determination of protein content

A known weight of fresh leaves (about 2 g) was homogenized in potassium phosphate buffer (50 mM, pH 7.4) containing 1 mM phenyl methyl sulfonyl fluoride, 2 mM dithiothreitol, 0.1 mM EDTA and 20% polyvinyl polypyrrolidone (PVPP) then centrifuged at 5000 ×g for 15 min. The protein content was determined spectrophotometrically in the supernatant (5 mL) using 5 mL of the protein reagent (100 mg of Coomassie Brilliant blue G-250 dissolved in 50 mL of 95% ethanol, then100 mL of 85% phosphoric acid were added and completed to 1 L with distilled water). The contents were mixed well and the absorbance at 595 nm was measured (Bradford, 1976) against a blank prepared from 100 µL of the appropriate buffer in addition to 5 ml of the protein reagent. The quantity of proteins was calculated from the standard curve using bovine albumin solution.

Determination of peroxidase and catalase activities

Enzymes were extracted from fresh leaves (5 g) by homogenization with 50 mM sodium phosphate buffer (pH 7.0) containing 1 mM EDTA and 0.5% PVPP under cold conditions. The extracts were centrifuged at 13000 ×g for 30 min at 4 °C and the supernatants were used as enzyme extracts. Catalase activity was assayed by following the consumption of H_2O_2 at 240 nm (Aebi, 1984) in 1 mL reaction mixture containing 50 mM sodium phosphate buffer (pH 7.0) and 10 mM H_2O_2. For each measurement, the reaction was initiated by adding the supernatant for the blank corresponds to the absorbance at zero time and the actual reading during the first 30 s and rates were calculated. Catalase specific activity was calculated as the enzyme amount that decomposes 1 µmol H_2O_2 min^{-1} mg^{-1} protein. The activity of ascorbate peroxidase was assayed following ascorbate oxidation by the decrement in absorption at 290 nm in a 1 mL reaction mixture containing 250 µM ascorbate, 50 mM potassium phosphate buffer (pH7.0), 0.5 mM EDTA and 1.5 mM H_2O_2 (Nakano & Asada, 1981) and the rate of decrease in absorbance was recorded. Ascorbate peroxidase specific activity was calculated as the enzyme amount that consumes 1 µmol ascorbate min^{-1} mg^{-1} protein.

Statistical analysis

The experiment was repeated twice and samples for each analysis were taken in triplicate from both experiments (n=6) and mean values (± SD) were applied. The experiment was designed as a complete randomized block consisting of 90 pots (5 sets for ZnO/SiO_2/GO treatments: control, 50, 150, 300 and 500 µg L^{-1}) x (3 sets for NaCl treatments: control, 100 mM, and 200 mM) x (3 replications) x (2 repetitions). The full data were subjected to two-way ANOVA followed by the LSD test at $p<0.05$.

Results

UV-Vis absorption spectroscopy was employed to confirm the successful incorporation of SiO_2 and ZnO NPs onto the rGO matrix, thereby verifying the synthesis of the final rGO/SiO_2/ZnO nanocomposite (NC) (Figure 1a). The absorption spectrum of pure rGO demonstrated minimal absorbance across the 200-500 nm range, with a slight, low-intensity increase below 250 nm characteristic of the $\pi \rightarrow \pi^*$ transitions in the C=C bonds of rGO. Conversely, the SiO_2 NPs exhibited a sharp, prominent absorption maximum at 240 nm, which is attributed to localized electronic transitions within the silica structure. The ZnO NPs displayed a distinctive, broad excitonic absorption band centered at 347 nm, which corresponds to the intrinsic direct band gap transition of ZnO. The absorption spectrum of the final NC clearly integrated the key features of the two incorporated oxides, confirming successful composite formation. Specifically, the NC spectrum displayed a distinct shoulder feature corresponding to the SiO_2 component near 245 nm and a major absorption peak at 345 nm, which is consistent with the characteristic ZnO excitonic absorption. A minor blueshift of the ZnO absorption peak from 347 nm in the pure nanoparticles to 345 nm in the NC was observed. This slight shift suggests a minimal modification in the electronic band structure of the ZnO component due to the intimate contact and synergistic interaction with the rGO and SiO_2 components. The overall integrated absorption

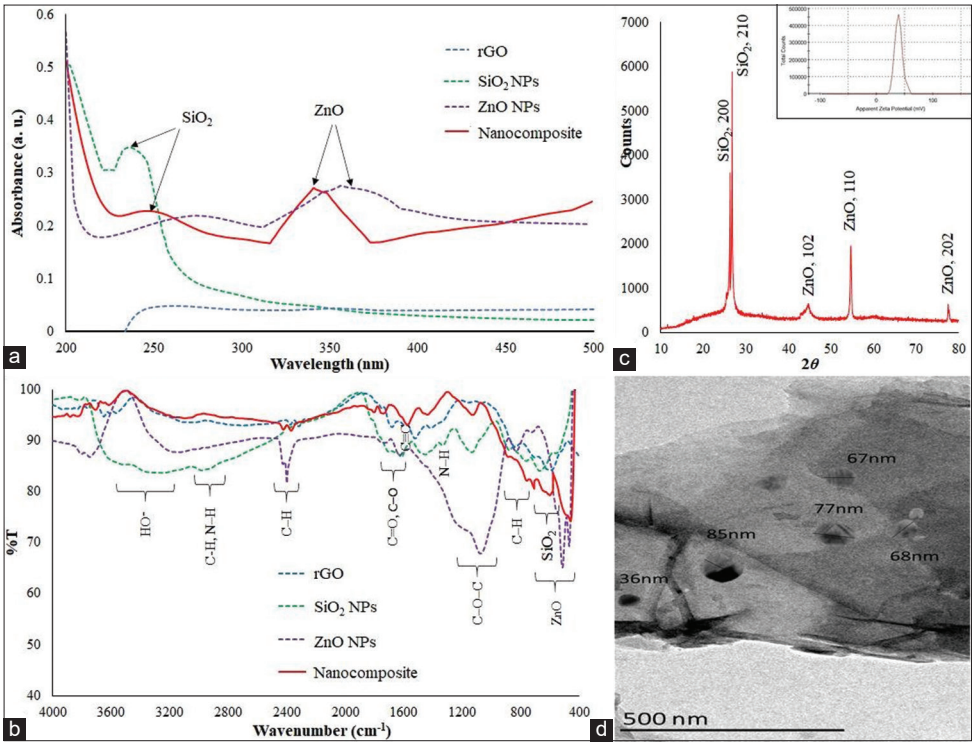

Figure 1: Characterization of the prepared nanomaterials. a) UV-Vis spectroscopy of rGO, SiO_2 NPs, ZnO NPs, and rGO/SiO_2/ZnO, b) FTIR spectroscopy of rGO, SiO_2 NPs, ZnO NPs, and rGO/SiO_2/ZnO, c) XRD spectrum and Zeta potential of rGO/SiO_2/ZnO and d) Transmission electron microscopic micrograph of rGO/SiO_2/ZnO. Scale bar=500 nm.

profile validates the co-existence and successful assembly of all three components into a single NC structure.

FTIR analysis was performed to verify the chemical integrity and bonding interactions among the components (Figure 1b). The spectrum of the ZnO NPs displayed a strong and sharp band at 440 cm^{-1}, which is definitely assigned to the Zn-O stretching vibration. The SiO_2 NPs spectrum was characterized by two main bands: an intense, broad absorption at 1080 cm^{-1} and a sharp band at 470 cm^{-1}, corresponding to the asymmetric stretching and bending modes of the Si-O-Si bridges, respectively. The rGO showed expected low-intensity peaks for residual O-H (3400 cm^{-1}) and C=C skeletal vibrations (1600 cm^{-1}). The FTIR spectrum of the nanocomposite successfully retained the key chemical fingerprints of all three constituents, specifically the strong Zn-O mode at 440 cm^{-1} and the characteristic Si-O-Si band at 1080 cm^{-1}. The simultaneous presence of these specific metal-oxygen and Si-oxygen vibrational bands confirms the successful chemical formation of the ternary composite material.

The XRD analysis confirmed the successful phase formation of all components within the nanocomposite (Figure 1c). The spectrum of the final rGO/SiO_2/ZnO nanocomposite exhibited all characteristic diffraction peaks of the highly crystalline hexagonal wurtzite ZnO phase (JCPDS card No. 00-036-1451), notably the high-intensity peaks at 2θ of 47.7°, 56.4°, and 77.2° corresponding to the (102), (110), and (202) planes, respectively. Additionally, the composite spectrum contained a broad hump between 20° and 26°, which is a combined signature of the amorphous SiO_2 structure and the disordered (002) stacking of the rGO sheets. Applying the Scherrer equation to the ZnO (110) and SiO2 (210) peaks yielded average crystallite sizes of ≈65.9 nm and ≈88.2 nm for the ZnO and SiO_2 components within the composite, confirming its nanoscale dimensions were successfully maintained. The Zeta potential measurement (Figure 1c), performed in the working medium, yielded a highly negative value of -32.8 mV. This strong magnitude of surface charge indicates that the synthesized rGO/SiO_2/ZnO material possesses excellent electrostatic stability when dispersed, a critical factor for preventing aggregation in colloidal systems.

The TEM micrograph (Figure 1d) shows the sheet-like morphology of the rGO matrix, with particles (ZnO and SiO_2) successfully anchored onto its surface. Measured particle sizes ranging from ≈36 nm to ≈85 nm confirm the composite's nanoscale architecture.

On the other hand, NaCl exerted its deleterious effects on soybean growth; 200 mM significantly reduced fresh and dry weights of soybean leaves, shoots and roots and also in leaf area, shoot height and root length, nonetheless, the decrease in water content was detected only in leaves but 100 mM seemed with no effect on all tested parameters (Figure 2). Meanwhile, fresh weight/dry weight ratio increased in roots by only 100 mM but unaffected in shoots and also in the ratios of root/shoot for both fresh weight and for length (Figure 3). In concomitant, 200 mM NaCl led to significant decreases in contents of phenolic compounds and protein and also in the activities of peroxidase and catalase, however, 100 mM NaCl exerted its significant decreases on only protein and catalase (Figure 4).

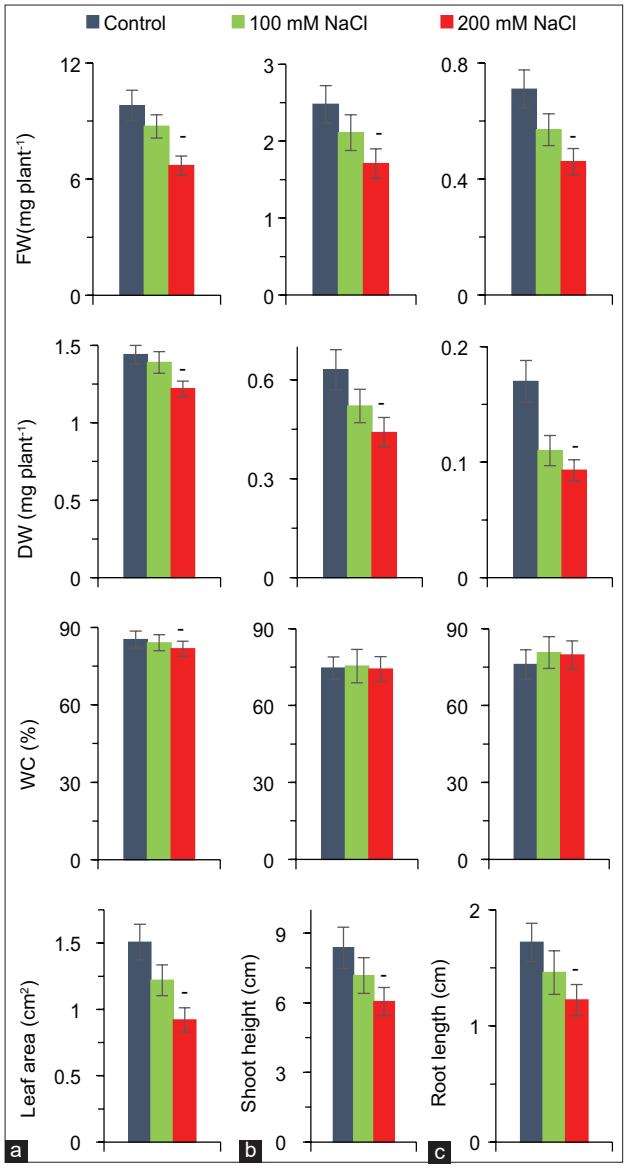

Figure 2: Changes in fresh weight, dry weight and water content of a) leaves, b) shoots and c) roots as well as leaf area, shoot height, and root length of 24-day old soybean seedlings subjected to NaCl treatment at 0, 100 and 200 mM. Data are means±SD of three independent replicates. Analysis of variance was performed followed by LSD test. Statistically significances are indicated as increase (+) or decrease (-), respectively at (p<0.05) relative to the untreated control

However, using the synthesized NC as seed priming at all concentrations was beneficial and effective for all tested parameters of soybean grown either under normal conditions (untreated control) or under NaCl-stress. The effectiveness under both conditions was most pronounced with the concentrations 150 and 300 µg L^{-1} while the influence of 50 µg L^{-1} was the least but 500 µg L^{-1} seemed depressive. With the untreated control, the NC significantly enhanced growth parameters, 50, 150 and 300 µg L^{-1} led to high values of fresh weight and dry weight of leaves, shoots and roots relative to those of the control as well as leaf area and the plant lengths with low changes in water content, however, these parameters were dropped with 500 µg L^{-1} (Figure 5). The NC, contrarily, slightly decreased root/shoot ratio for fresh weight and for length but these ratios were unaffected by the highest concentration (Figure 6). Moreover, the NC at 50, 150 and 300 µg L^{-1} significantly enhanced phenolics, protein and activities of peroxidase and catalase while 500 µg L^{-1} led to decreases (Figure 7). Anyway, these enhancements/improvements of all tested parameters -if any- were higher with 150 and 300 µg L^{-1} followed by 50 but the highest concentration (500 µg L^{-1}) did not assist these parameters.

Whilst under NaCl treatments, utilizing the NC as seed priming led to great mitigation of the NaCl-induced negative effects of all tested parameters. Moreover, the application of the NC significantly enhanced fresh weight, dry weight and water content of leaves, shoots and roots and also in leaf area and lengths of shoots and roots; more enhancements were induced by the concentrations 150 and 300 µg L^{-1} with least efficiency of 50 µg L^{-1} but 50 µg L^{-1} synergized the impacts of salinity (Figure 5). Similar effects were induced in ratios of fresh weight/dry weight in shoots and roots whereas the ratios of root/shoot for either fresh weight or lengths seemed less affected (Figure 6). Moreover, the NC particularly at 150 and 300 µg L^{-1} led to significant increments in phenolics, protein and activities of peroxidase and catalase (Figure 7). As a whole, the NC at the concentrations 150 and 300 µg L^{-1} were most effective in mitigating the impacts of NaCl at 100 and 200 mM and moreover exhibited some increments in the tested parameters. Although neither the 50 nor 500 µg L^{-1} concentration exhibited increments in most parameters under 200 mM NaCl, the smallest concentration had somewhat positive effects in alleviating the influence of this salinity level but with a lesser efficiency relative to the concentrations 150 and 300 µg L^{-1} but the highest concentration was troublesome to soybean.

Discussion

Given the importance of soybeans in Egypt, as it is the most important source of proteins and vegetable oils (Budran *et al.,* 2023), and given that it is insufficient to meet the demand, it is suggested that expanding their cultivation stands out as an effective agricultural solution to address the challenges of food security, import reliance, and economic diversification (Naser *et al.,* 2024). For these reasons, and especially since the agricultural area is limited, despite the existence of vast areas neglected due to their salinity, which makes them unsuitable for growing salt-intolerant crops, therefore, utilizing this saline soil to grow this staple crop, while enhancing its ability to tolerate salinity and mitigating its effects, is a promising strategy for increasing food productivity, and thus the food gap can be overcome.

Without mitigating its impacts, salinity disrupts several processes in plants due to the alteration of water potential, causing ion imbalance and toxicity, impairing cell division and expansion, and generating reactive oxygen species (ROS) (Badran *et al.,* 2015; Nemat Alla & Hassan, 2019), which further damage cellular components (Nemat Alla *et al.,* 2020). In the present work, the detrimental impacts of NaCl were evident in the reduction of soybean growth and other parameters. These impacts on soybean have to be overcome to withstand harsh conditions. Nanoparticles (NPs) emerge as an efficient solution in this field. Thus an attempt was made in

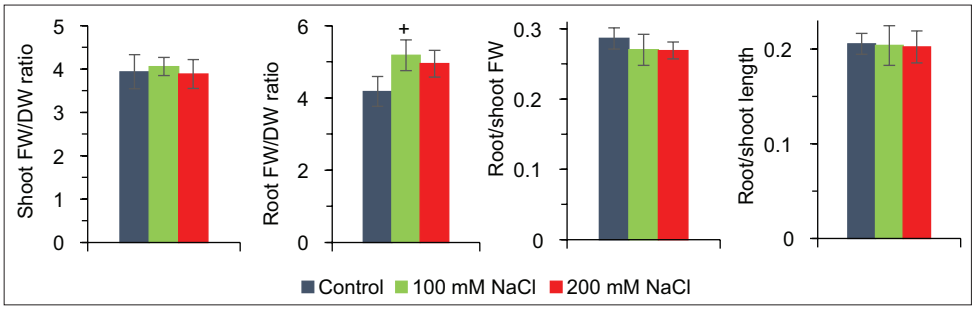

Figure 3: Changes in fresh weight/dry weight ratio of both shoot and root and on root/shoot ratio of both fresh weight and length of 24-day old soybean subjected to NaCl treatment at 0, 100 and 200 mM. Data are means±SD of three independent replicates. Analysis of variance was performed followed by LSD test. Statistically significances are indicated as increase (+) or decrease (-), respectively at (p<0.05) relative to the untreated control

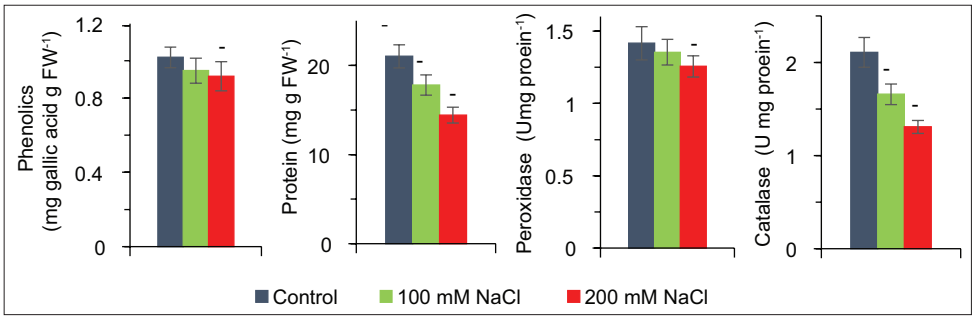

Figure 4: Changes in contents of phenolics and protein and the specific activity of peroxidase and catalase of 24-day old soybean subjected to NaCl treatment at 0, 100 and 200 mM. Data are means±SD of three independent replicates. Analysis of variance was performed followed by LSD test. Statistically significances are indicated as increase (+) or decrease (-), respectively at (p<0.05) relative to the untreated control

this work to utilize SiO_2, ZnO, and rGO NPs in combination with soybean extract for the synthesis of a safe and effective nanocomposite (NC), rGO/SiO_2/ZnO, to accomplish what is required about tolerating soybean to salinity impacts.

The successful construction of the rGO/SiO_2/ZnO ternary NC was evidenced by the UV-Vis absorption spectroscopy confirming the co-existence of its photoactive and stabilizing components. The pure ZnO NPs exhibited a sharp excitonic absorption maximum at 347 nm, a characteristic signature of ZnO (El-Nour *et al.,* 2023). Based on this wavelength, the corresponding direct band gap energy (Eg) was calculated to be ≈3.57 eV. This value is notably higher than the bulk ZnO band gap (≈ 3.37 eV), providing clear spectroscopic confirmation of the quantum confinement effect, which arises from the synthesis of ZnO crystallites smaller than their Bohr exciton radius (Musa & Qamhieh, 2019). Upon integration into the final NC structure, the ZnO absorption peak experienced a slight blueshift to 345 nm, corresponding to a marginal increase in Eg to 3.59 eV. This minor shift suggests that the primary electronic structure of the ZnO core particles is well-preserved. While significant redshifts are often expected in carbon-semiconductor composites due to defect states extending into the visible region, the observed negligible shift indicates that the electronic influence of rGO does not significantly alter the bulk ZnO band gap but rather focuses on the crucial interfacial boundaries (El-Zahed *et al.,* 2024).

The FTIR results reinforce the structural stability and successful chemical assembly of the NC. The retention of the distinctive Si-O-Si and Zn-O stretching modes in the composite spectrum confirms that all components maintain their core chemical identity. The significance of the SiO_2 component is highlighted here: it is structurally incorporated, as confirmed by its characteristic 1080 cm^{-1} bands. This inert material functions as a structural spacer, utilizing its surface functionality (such as the residual hydroxyl groups) to provide anchor points that physically separate the ZnO NPs and the rGO sheets (Zhao *et al.,* 2017). This stabilization effect is crucial, as it prevents the aggregation of the ZnO NPs and the restacking of the rGO sheets, thus maximizing the exposed active surface area and the interfacial contact zone (Kang *et al.,* 2016). The combined structural analysis from XRD and FTIR conclusively verifies the formation of the desired rGO/SiO_2/ZnO ternary NC. The XRD data confirmed that the ZnO maintains its phase-pure, highly crystalline wurtzite structure, and the small change in crystallite size (≈65.9 nm to 64.7 nm) demonstrates that the synthetic methodology successfully inhibited crystal growth (Wu *et al.,* 1999).

This structural synergy is directly supported by the highly negative Zeta potential (-32.8 mV). This strong surface charge, primarily contributed by the highly negative rGO and SiO_2 surfaces, ensures superior colloidal stability, guaranteeing that the material remains well-dispersed and active under operating conditions (Zhang *et al.,* 2023). This strong negative magnitude exceeds the conventional stability threshold of 30 mV, indicating excellent electrostatic stability and a low tendency for particle aggregation in the aqueous medium (Fayed *et al.,* 2024). In addition, the

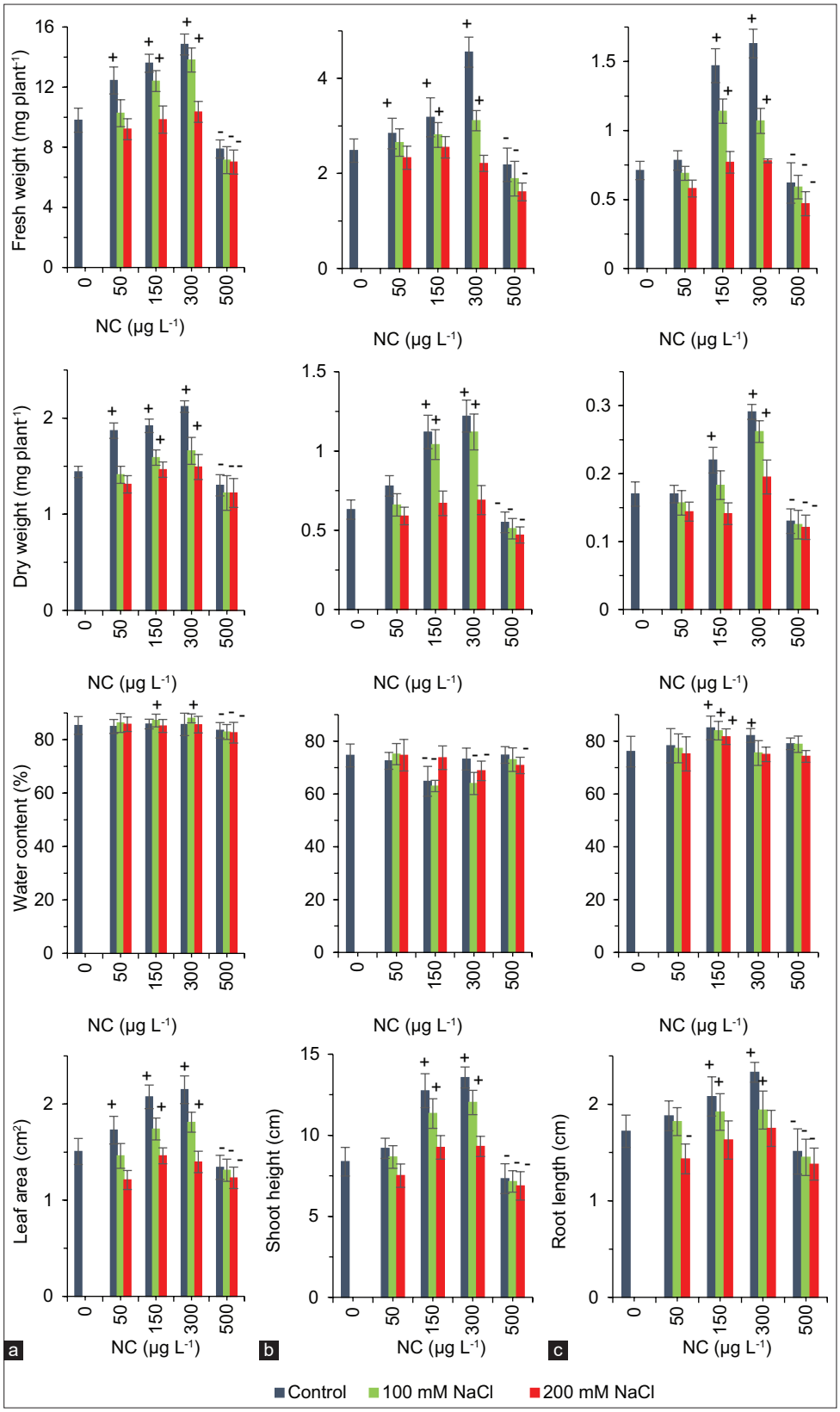

Figure 5: Influence of priming soybean seeds in the synthesized nanocomposite, rGO/SiO_2/ZnO, on fresh weight, dry weight and water content of a) leaves, b) shoots and c) roots as well as leaf area, shoot height, and root length of 24-day old seedlings subjected to NaCl treatment at 0, 100 and 200 mM. Data are means±SD of three independent replicates. Two-way ANOVA was performed followed by LSD test. Statistically significances are indicated as increase (+) or decrease (-), respectively at (p<0.05) relative to the untreated control

TEM characterization data therefore confirms the successful engineering of a phase-pure, well-dispersed, and structurally stable rGO/SiO_2/ZnO ternary NC.

This NC was synthesized to be used as seed priming for alleviating the indicated impacts of salinity on soybean. Utilizing this NC appeared very useful for soybean grown

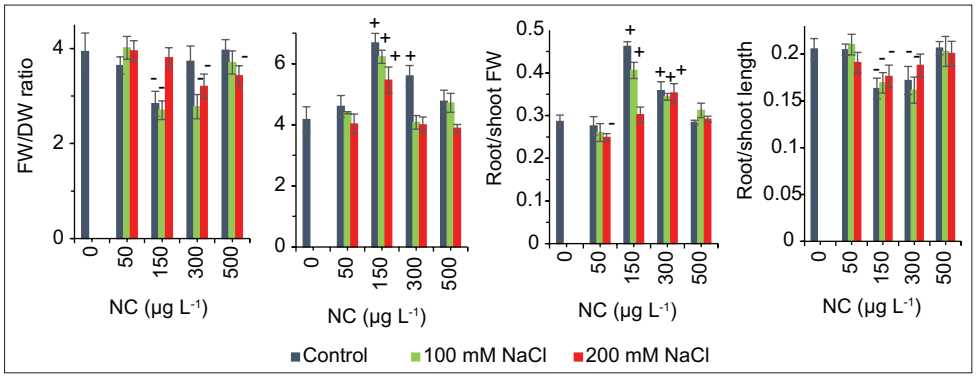

Figure 6: Influence of priming soybean seeds in the synthesized nanocomposite, rGO/SiO_2/ZnO, on fresh weight/dry weight ratio of both shoot and on root and root/shoot ratio of both fresh weight and length of 24-day old seedlings subjected to NaCl treatment at 0, 100 and 200 mM. Data are means±SD of three independent replicates. Two-way ANOVA was performed followed by LSD test. Statistically significances are indicated as increase (+) or decrease (-), respectively at (p<0.05) relative to the untreated control

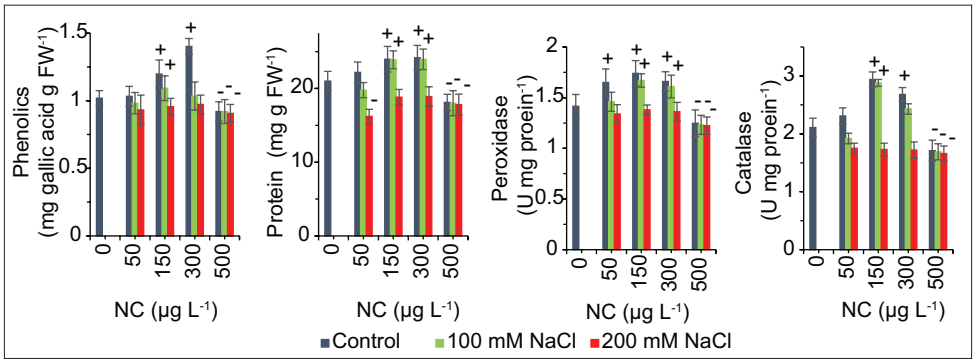

Figure 7: Influence of priming soybean seeds in the synthesized nanocomposite, rGO/SiO_2/ZnO, on contents of phenolics and protein and activities of peroxidase and catalase of 24-day old seedlings subjected to NaCl treatment at 0, 100 and 200 mM. Data are means±SD of three independent replicates. Two-way ANOVA was performed followed by LSD test. Statistically significances are indicated as increase (+) or decrease (-), respectively at (p<0.05) relative to the untreated control

either in the normal conditions (control) or under NaCl stress. Under normal conditions, the NC greatly ameliorated growth parameters, contents of phenolics and protein and the activities of peroxidase and catalase. Among the concentrations used, 150 and 300 µg L^{-1} were more effective than 50 µg L^{-1} while 500 µg L^{-1} was not the case. However, the NC under NaCl stress mitigated the induced deleterious impacts; greater was the mitigation with the concentrations 150 and 300 µg L^{-1} in relation to 50 µg L^{-1}. The increased fresh and dry weights by the NC point to an improved capacity of soybean to ameliorate its vital processes. The beneficial effect of the NC in the present work is supported by the benefits of its NPs components. Si is a critical component of crop production, and alleviates toxic effects caused by various stresses in plants especially in minimizing the negative impacts of oxidative, salinity, and drought stresses (Seleiman *et al.,* 2019). SiO_2 provides stress tolerance and boosts photosynthesis. Besides, Zn supports enzymatic functions and ion homeostasis (Alsafran *et al.,* 2022). ZnO NPs importance arises from its necessity for the activity of various enzymes and from its roles in repair process of photo system II. GO offers significant potential for improving agricultural practices due to its unique properties and ability to enhance plant growth, nutrient absorption, and stress tolerance (Yang *et al.,* 2025). It can act as a fertilizer, a smart delivery system for nutrients and pesticides, and a tool for improving soil health as well as enhancing the antimicrobial properties (Baka & El-Zahed, 2023) and improves chlorophyll content and water retention (Safkhan *et al*., 2018).

In consistence, the plant length showed improvements and also water status was modulated referring to overcoming the NaCl-induced dehydration. In this account, Sarioğlu (2025) indicated that salinity leads to dehydration. However, Daraei *et al.* (2024) concluded that NPs can improve a plant's ability to retain water. So, this NC with concentrations (50-300 µg L^{-1}) seemed to maximize soybean tolerance under stress conditions. This suggestion is confirmed from the increases in protein that would rise the enzymes necessary for several processes and so increasing the plant biomass as indicated. In concomitant, phenolics and activities of peroxidase and catalase were stimulated to boost the antioxidant system in the plant with the scavenging of ROS and thus eliminate oxidative stress. In this respect, Junedi *et al.* (2023) concluded that NPs mitigate salinity stress in plants by enhancing antioxidant defense. Specifically, NPs like ZnO and Si boosting the activity of antioxidant enzymes (Gheisary & Fattahi, 2025) leading to less oxidative damage and improved plant performance under saline conditions. This interaction boosts the enzymes' activity, which increases the scavenging of ROS and reduces oxidative damage.

Nile *et al.* (2022) indicated that nanopriming can induce the formation of nanopores in shoots, increase the expression of aquaporin genes, and speed up starch hydrolysis, all of which promote germination and early growth. Nanopriming can also reduce the negative effects of salt stress by decreasing harmful compounds like malondialdehyde and electrolyte leakage and can stimulate the production of antioxidant enzymes, which help protect the plant from damage (Yang *et al.,* 2024). Therefore, the NC can improve plant growth by acting as a nanoprimer to enhance seed germination and increasing nutrient uptake to cope with stress (do Espirito Santo Pereira *et al.,* 2021). Accordingly, the present work indicates that salinity disrupts growth, phenolics, protein and activities of catalase and peroxidase while the application of the synthesized NC completely eliminated these disruptions and even induced some improvements. The inclusion of ZnO, SiO_2, and GO in the NC likely contributed to improved plant health because of their advantageous benefits. Shoukat *et al.* (2025) stated that Si-Zn nanocomposites increased maize yield.

Therefore, the synthesized NC NPs is particularly useful under salt stress for combining nutrient delivery with stress mitigation giving rise to improving soybean growth synchronized with elevated protein and ameliorated antioxidant performance revealing modulation of soybean salinity tolerance particularly at the concentrations 150 to 300 μg L^{-1}, however, 50 μg L^{-1} although inducing some ameliorations, it is insufficient to exert its action whereas 50 μg L^{-1} was too much to reveal some toxicity.

Conclusions

The importance of soybeans necessitates searching for increasing its productivity through enlarging its cultivation utilizing the huge areas of the neglected saline soils but with assistance of an external supporter to mitigate salinity impacts. In this work, the rGO/SiO_2/ZnO nanocomposite (NC) was successfully synthesized from reduced graphene oxide, silicon dioxide, and zinc oxide NPs in combination with soybean extract to be used as seed priming for mitigating salinity stress. This NC is characterized with an absorption peak at 354 nm, indicating to the annealing of SiO_2 and ZnO NPs on the GO sheets with a positive charge (+30.9±10.4 mV). The NPs seemed as rod-shaped particles with an average size ranging from 64 to 78 nm. NaCl negatively impacted growth parameters, phenolics, protein and activities of peroxidase and catalase; however, using the synthesized NC at 50 to 300 μg L^{-1} highly mitigated these impacts and moreover, great ameliorations were induced. The most effective concentrations of the NC were 150 and 300 μg L^{-1} while 50 μg L^{-1} was less effective because it seemed insufficient to exert its action; whereas 500 μg L^{-1} appeared too much to synergize the impacts of salinity. These findings conclude that this NC is a highly promising safe and efficient protectant for enhancing soybean's resilience and enabling its cultivation in saline soils when used at the concentrations of 150 and 300 μg L^{-1}. Herein, the novelty of the rGO/SiO_2/ZnO NC tri-component architecture as a safe and efficient seed priming agent has been demonstrated. This knowledge can be implemented for future research for understanding the interference of the NC within plant cells and coordinating the responses of the plant to modulations in mechanisms of NaCl tolerance.

Author contributions

Mamdouh M. Nemat Alla, Enas G. Badran and Mohamed M. El-Zahed: planed the scientific experiments; Mamdouh M. Nemat Alla and Nemat M. Hassan: performed data analysis and wrote, edited and reviewed the manuscript; Enas G. Badran, Manal A. Abdelhamid and Mohamed M. El-Zahed: performed the experiments. All authors have reviewed the completed manuscript and given consent for its publication, indicating their agreement with the content and findings reported in the study.

References

Aebi, H. (1984). Catalase *in vitro*. *Methods in Enzymology, 105*, 121-126. https://doi.org/10.1016/S0076-6879(84)05016-3

Al-Azawi, M. T., Hadi, S. M., & Mohammed, C. H. (2019). Synthesis of silica nanoparticles via green approach by using hot aqueous extract of *Thuja orientalis* leaf and their effect on biofilm formation. *Iraqi Journal of Agricultural Sciences, 50*, 245-255. https://doi.org/10.36103/ijas.v50iSpecial.196

Alsafran, M., Usman, K., Ahmed, B., Rizwan, M., Saleem, M. H., & Al Jabri, H. (2022). Understanding the phytoremediation mechanisms of potentially toxic elements: A proteomic overview of recent advances. *Frontiers in Plant Science, 13*, 881242. https://doi.org/10.3389/fpls.2022.881242

Asadi, M., Nasiri, Y., Rasouli, F., Kakaei, K., Morshedloo, M. R., Ercisli, S., Skrovankova, S., & Mlcek, J. (2025). Application of graphene oxide nanoparticles for improvement of growth parameters, photosynthetic pigments, and essential oil quality and yield of *Lavandula angustifolia* Mill. under green manure incorporation. *BMC Plant Biology, 25*, 1278. https://doi.org/10.1186/s12870-025-07364-2

Badran, E. G., Abogadallah, G. M., Nada, R. M., & Nemat Alla, M. M. (2015). Role of glycine in improving the ionic and ROS homeostasis during NaCl stress in wheat. *Protoplasma, 252*, 835-844. https://doi.org/10.1007/s00709-014-0720-2

Baka, Z. A., & El-Zahed, M. M. (2023). Biocontrol of chocolate spot disease of broad bean (*Vicia faba* L.) caused by *Botrytis fabae* using biosynthesized reduced graphene oxide/silver nanocomposite. *Physiological and Molecular Plant Pathology, 127*, 102116. https://doi.org/10.1016/j.pmpp.2023.102116

Bradford, M. M. (1976). A rapid and sensitive method for the quantitation of microgram quantities of protein utilizing the principle of protein-dye binding. *Analytical Biochemistry, 72*(1-2), 248-254. https://doi.org/10.1016/0003-2697(76)90527-3

Budran, E. G., Abdelhamid, M. A., Hassan, N. M., & Nemat Alla, M. M. (2023). Ameliorative effect of ascorbate on growth and oil fatty acid composition of soybean under salinity. *Egyptian Journal of Botany, 63*, 635. https://doi.org/10.21608/ejbo.2023.173612.2198

Daraei, E., Bayat, H., & Zamani, P. (2024). Effects of metal oxide nanoparticles on soil water retention curve and tensile strength. *Pedosphere, 34*(6), 1136-1145. https://doi.org/10.1016/j.pedsph.2023.07.017

do Espirito Santo Pereira, A., Caixeta Oliveira, H., Fernandes Fraceto, L., & Santaella, C. (2021). Nanotechnology potential in seed priming for sustainable agriculture. *Nanomaterials, 11*(2), 267. https://doi.org/10.3390/nano11020267

El-Nour, A. T. A., Abou-Dobara, M. I., El-Sayed, A. K. A., & El-Zahed, M. M. (2023). Antibacterial activity of optimized extracellular biosynthesized zinc oxide nanoparticles using *Corynebacterium sp*. ATCC 6931. *Scientific Journal for Damietta Faculty of Science, 13*(3), 63-70. https://doi.org/10.21608/sjdfs.2023.231788.1129

El-Zahed, M. M., Abou-Dobara, M. I., El-Khodary, M. M., & Mousa, M. M. A. (2024). Antimicrobial activity and nanoremediation of heavy metals using biosynthesized CS/GO/ZnO nanocomposite by *Bacillus subtilis* ATCC 6633 alone or immobilized in a macroporous cryogel. *Microbial Cell Factories, 23*, 278. https://doi.org/10.1186/s12934-024-02535-6

Fayed, R. M., Baka, Z. A. M., & El-Zahed, M. M. (2024). Antibacterial activity of green synthesized zinc oxide nanoparticles using *Washingtonia robusta* H. Wendl fruit extract. *Scientific Journal for Damietta Faculty of Science, 14*(3), 90-101. https://doi.org/10.21608/sjdfs.2025.332686.1193

Geremew, A., Stovall, L., Woldesenbet, S., Ma, X., & Carson, L. (2025). Nanopriming with zinc oxide: a novel approach to enhance germination and antioxidant systems in amaranth. *Frontiers in Plant Science, 16*, 1599192. https://doi.org/10.3389/fpls.2025.1599192

Gheisary, B., & Fattahi, M. (2025). Selenium and zinc oxide nanoparticles stimulate product quality, phenolic content, antioxidant activity, and shikonin production in Italian bugloss (*Echium italicum* L) plantlets under *in vitro* conditions. *BMC Plant Biology, 25*, 1465. https://doi.org/10.1186/s12870-025-07461-2

Hofmann, T., Lowry, G. V., Ghoshal, S., Tufenkji, N., Brambilla, D., Dutcher, J. R., Gilbertson, L. M., Giraldo, J. P., Kinsella, J. M., Landry, M. P., Lovell, W., Naccache, R., Paret, M., Pedersen, J. A., Unrine, J. M., White, J. C., & Wilkinson, K. J. (2020). Technology readiness and overcoming barriers to sustainably implement nanotechnology-enabled plant agriculture. *Nature Food, 1*, 416-425. https://doi.org/10.1038/s43016-020-0110-1

Jafari, A. J., Kalantary, R. R., Esrafili, A., & Arfaeinia, H. (2018). Synthesis of silica-functionalized graphene oxide/ZnO coated on fiberglass and its application in photocatalytic removal of gaseous benzene. *Process Safety and Environmental Protection, 116*, 377-387. https://doi.org/10.1016/j.psep.2018.03.015

Junedi, M. A., Mukhopadhyay, R., & Manjari, K. S. (2023). Alleviating salinity stress in crop plants using new engineered nanoparticles (ENPs). *Plant Stress, 9*, 100184. https://doi.org/10.1016/j.stress.2023.100184

Kang, W., Jimeng, X., & Xitao, W. (2016). The effects of ZnO morphology on photocatalytic efficiency of ZnO/RGO nanocomposites. *Applied Surface Science, 360*, 270-275. https://doi.org/10.1016/j.apsusc.2015.10.190

Maroni, F., Raccichini, R., Birrozzi, A., Carbonari, G., Tossici, R., Croce, F., Marassi, R., & Nobili, F. (2014). Graphene/silicon nanocomposite anode with enhanced electrochemical stability for lithium-ion battery applications. *Journal of Power Sources, 269*, 873-882. https://doi.org/10.1016/j.jpowsour.2014.07.064

Mohamed, I. A. A., Foda, M. F., Khan, I. U., Batool, M., Awad-Allah, E. F. A., Fan, C., Fu, C., Wang, J., Yin, Z., & Wu, H. (2025). Nano-improved plant salinity tolerance: The importance of K^+/Na^+ homeostasis and crosstalk between Ca^{2+} and hormones. *Plant Nano Biology, 13*, 100196. https://doi.org/10.1016/j.plana.2025.100196

Musa, I., & Qamhieh, N. (2019). Study of optical energy gap and quantum confinment effects in Zinc Oxide nanoparticles and nanorods. *Digest Journal of Nanomaterials and Biostructures, 14*(1), 119.

Nakano, Y., & Asada, k. (1981). Hydrogen peroxide is scavenged by ascorbate specific peroxide in spinach chloroplast. *Plant and Cell Physiology, 22*(5), 867-880. https://doi.org/10.1093/oxfordjournals.pcp.a076232

Naseem, A., Iqbal, S., Jabeen, K., Umar, A., Alharbi, K., Antar, M., Grądecka-Jakubowska, K., Gancarz, M., & Ali, I. (2023). Organic amendments improve salinity-induced osmotic and oxidative stress tolerance in Okra (*Abelmoschus esculentus* (L.)Moench). *BMC Plant Biology, 23*, 522. https://doi.org/10.1186/s12870-023-04527-x

Naser, M., Abdelghany, A. M., Wu, T., Sun, S., & Tianfu, H. (2024). Soybean in Egypt: current situation, challenges, and future perspectives. *Discover Sustainability, 5*, 425. https://doi.org/10.1007/s43621-024-00656-x

Nemat Alla, M. M., & Hassan, N. M. (2019). Alleviation of chlorimuron-ethyl toxicity to soybean by branched-chain amino acids or naphthalic anhydride. *Rendiconti Lincei. Scienze Fisiche e Naturali, 30*, 759-766. https://doi.org/10.1007/s12210-019-00838-0

Nemat Alla, M., Budran, E. G., Mohammed, F. A., Hassan,N. M., & Abdelhamid, M. A. (2020). Overexpression of Na^+-manipulating genes in wheat by selenium is associated with antioxidant enforcement for enhancement of salinity tolerance. *Rendiconti Lincei. Scienze Fisiche e Naturali, 31*, 177-187. https://doi.org/10.1007/s12210-019-00868-8

Nile, S. H., Thiruvengadam, M., Wang, Y., Samynathan, R., Shariati, M. A., Rebezov, M., Nile, A., Sun, M., Venkidasamy, B., Xiao, J., & Kai, G. (2022). Nano-priming as emerging seed priming technology for sustainable agriculture-recent developments and future perspectives. *Journal of Nanobiotechnology, 20*, 254. https://doi.org/10.1186/s12951-022-01423-8

Ochoa-Chaparro, E. H., Patiño-Cruz, J. J., Anchondo-Páez, J. C., Pérez-Álvarez, S., Chávez-Mendoza, C., Castruita-Esparza, L. U., Márquez, E. M., & Sánchez, E. (2025). Seed nanopriming with ZnO and SiO_2 enhances germination, seedling vigor, and antioxidant defense under drought stress. *Plants, 14*(11), 1726. https://doi.org/10.3390/plants14111726

Qin, P., Wang, T., & Luo, Y. (2022). A review on plant-based proteins from soybean: Health benefits and soy product development. *Journal of Agriculture and Food Research, 7*, 100265. https://doi.org/10.1016/j.jafr.2021.100265

Rastogi, A., Tripathi, D. K., Yadav, S., Chauhan, D. K., Zivcak, M., Ghorbanpour, M., El- Sheery, N. I., & Brestic, M. (2019). Application of silicon nanoparticles in agriculture. *3 Biotech, 9*, 90. https://doi.org/10.1007/s13205-019-1626-7

Rehman, A., Khan, S., Sun, F., Peng, Z., Feng, K., Wang, N., Jia, Y., Pan, Z., He, S., Wang, L., Qayyum, A., Du, X., & Li, H. (2024). Exploring the nano-wonders: unveiling the role of nanoparticles in enhancing salinity and drought tolerance in plants. *Frontiers in Plant Science, 14*, 1324176. https://doi.org/10.3389/fpls.2023.1324176

Safkhan, S., Chaichi, M. R., Khoshbakht, K., Amini, A., & Motesharezadeh, B. (2018). Application of nano material grapheme oxide on biochemical traits of Milk thistle (*Silybum marianum* L.) under salinity stress. *Australian Journal of Crop Science, 12*(6), 931-936.

Sarioğlu, A. (2025). Growth of soybean plants under saline conditions: the role of potassium and *Bradyrhizobium japonicum* inoculation. *BMC Plant Biology, 25*, 473. https://doi.org/10.1186/s12870-025-06477-y

Seleiman, M. F., Refay, Y., Al-Suhaibani, N., Al-Ashkar, I., El-Hendawy, S., & Hafez, E. M. (2019). Integrative effects of rice-straw biochar and silicon on oil and seed quality, yield

and physiological traits of *Helianthus annuus* L. grown under water deficit stress. *Agronomy,* 9(10), 637. https://doi.org/10.3390/agronomy9100637

Shah, S. S., Li, Z., Yan, H., Shi, L., & Zhou, B. (2020). Comparative study of the effects of salinity on growth, gas exchange, N accumulation and stable isotope signatures of forage oat (*Avena sativa* L.) genotypes. *Plants, 9*(8), 1025. https://doi.org/10.3390/plants9081025

Shoukat, A., Maryam, U., Pitann, B., Zafar, M. M., Nawaz, A., Hassan, W., Seleiman, M. F., Saqib, Z. A., & Mühling, K. H. (2025). Efficacy of nano and conventional zinc and silicon fertilizers for nutrient use efficiency and yield benefits in maize under saline field conditions. *Plants, 14*(15), 673. https://doi.org/10.3390/plants14050673

Singleton, V. L., & Rossi, J. A. (1956). Colorimetry of total phenolics with phosphomolybdic-phosphotungestic acid reagents. *American Journal of Enology and Viticulture, 16*(3), 144-158. https://doi.org/10.5344/ajev.1965.16.3.144

Tripathi, D., Nam, A., Oldenburg, D. J., & Bendich, A. J. (2020). Reactive oxygen species, antioxidant agents, and DNA damage in developing maize mitochondria and plastids. *Frontiers in Plant Science, 11*, 596. https://doi.org/10.3389/fpls.2020.00596

Umar, H., Kavaz, D., & Rizaner, N. (2019). Biosynthesis of zinc oxide nanoparticles using *Albizia lebbeck* stem bark, and evaluation of its antimicrobial, antioxidant, and cytotoxic activities on human breast cancer cell lines. *International Journal of Nanomedicine, 14*, 87-100.

Wu, N.-L., Wang, S.-Y., & Rusakova, I. A. (1999). Inhibition of crystallite growth in the sol-gel synthesis of nanocrystalline metal oxides. *Science, 285*(5432), 1375-1377. https://doi.org/10.1126/science.285.5432.1375

Yang, L., Zhang, L., Zhang, Q., Wei, J., Zhao, X., Zheng, Z., Chen, B., & Xu, Z. (2024). Nanopriming boost seed vigor: Deeper insights into the effect mechanism. *Plant Physiology and Biochemistry, 214*, 108895. https://doi.org/10.1016/j.plaphy.2024.108895

Yang, Y., Ye, C., Zhao, M., Li, J., Zhang, X., Yang, Z., Yang, Z., Algopishi, U. B., & Ahmed, W. (2025). Nanoparticles in sustainable agriculture: enhancing nutrient use efficiency and abiotic stress resilience under climate change. *Plant Stress, 17*, 100982. https://doi.org/10.1016/j.stress.2025.100982

Zhan, Q., Ahmad, A., Arshad, H., Yang, B., Chaudhari, S. K., Batool, S., Hasan, M., Feng, G., Mustafa, G., & Hatami, M. (2024). The role of reduced graphene oxide on mitigation of lead phytotoxicity in *Triticum aestivum* L. plants at morphological and physiological levels. *Plant Physiology and Biochemistry, 211*, 108719. https://doi.org/10.1016/j.plaphy.2024.108719

Zhang, R., Li, J., Jerrams, S., Hu, S., Liu, L., Wen, S., & Zhang, L. (2023). Constructing a fine dispersion and chemical interface based on an electrostatic self-assembly and aqueous phase compound in GO/SiO_2/SBR composites to achieve high-wear resistance in eco-friendly green tires. *Chemical Engineering Journal, 452*, 139113. https://doi.org/10.1016/j.cej.2022.139113

Zhao, Y., Liu, L., Cui, T., Tong, G., & Wu, W. (2017). Enhanced photocatalytic properties of ZnO/reduced graphene oxide sheets (rGO) composites with controllable morphology and composition. *Applied Surface Science, 412*, 58-68. https://doi.org/10.1016/j.apsusc.2017.03.207